phys. stat. sol. (b) **212**, 207 (1999)

Subject classification: 78.55.Hx; 63.20.Kr; 71.70.Ch; S11

Luminescence and Its Temperature Effects on Sm^{2+} in Alkaline Earth Borates

QINGHUA ZENG[1]) (a), ZHIWU PEI (a), QIANG SU (a), and SHIHUA HUANG (b)

(a) Laboratory of Rare Earth Chemistry and Physics, Changchun Institute of Applied Chemistry, Chinese Academy of Sciences, Changchun 130022, People's Republic of China

(b) Laboratory of Excited State Processes, Chinese Academy of Sciences, Changchun 130021, People's Republic of China

(Received June 26, 1998; in revised form November 25, 1998)

The luminescence of Sm^{2+} in alkaline earth borates (BaB_8O_{13}, SrB_4O_7 and SrB_6O_{10}) is reported. The temperature effects on luminescence and decay time of Sm^{2+} are studied. Due to the thermal population, $^5D_1 \rightarrow {}^7F_J$ transitions of Sm^{2+} in BaB_8O_{13}, SrB_4O_7 and SrB_6O_{10} are observed at room temperature. The f–d broad emission transitions of Sm^{2+} in SrB_4O_7 and SrB_6O_{10} are observed at high temperature whereas no f–d transition is observed in BaB_8O_{13}.

1. Introduction

An excited impurity ion in the lattice can lose its energy by spontaneous phonon, or phonon-assisted emission, or non-radiative transitions. They are temperature-dependent and arise from vibration–electronic or 'vibronic' interactions. Vibronic transitions of rare-earth ions arise from the coupling of the $4f^n$ state with the infrared-active vibrational modes (electron–phonon coupling) of the lattice in which the parity selection rule of the purely electronic f–f transitions is broken. The electron–phonon coupling strength is usually the main reason for the admixture of states having opposite parity [1 to 3]. Such coupling with 4f electrons is mostly weak due to the well shielding by the outer $5s^25p^6$ electrons, but it has a large influence on the optical properties of rare-earth ions. This interaction manifests itself in several ways, such as static interaction and dynamic interaction [4]. The static interaction results in the crystal-field splitting of the $^{2S+1}L_J$ terms. The dynamic interaction results in multiphonon relaxation, vibronic transitions and temperature-dependent line broadening and line shifts. The relative contributions of the vibronic and purely radiative transitions to the decay can be found directly by measuring the fluorescence lines as a function of temperature.

In this paper, the luminescence and its temperature effects for Sm^{2+} ($4f^6$) in some alkaline earth borates are reported. Since no detailed structure was reported for BaB_8O_{13} and SrB_6O_{10} so far [5, 6], we therefore use the luminescence, especially the $^5D_0 \rightarrow {}^7F_0$ transition of Sm^{2+} as structural probe to study the crystallographic site of cations (Ba^{2+}, Sr^{2+} or Sm^{2+}) in hosts.

[1]) Corresponding author.

2. Experimental

Samples of BaB_8O_{13}, SrB_4O_7 and SrB_6O_{10} doped with rare-earth ions were prepared by an intimate mixture of analytical-grade barium (strontium) carbonates, boric acid (3 mol% excess). The concentration of the dopant Sm_2O_3 (99.99%) is 2 mol% of Ba^{2+} (Sr^{2+}) ions. The samples were heated in H_2/N_2 for 5 h.

The crystal structure was checked by X-ray powder diffraction using CuKα_1 radiation with a Rigaku Model D/Max-IIB diffractometer at 40 kV, 2°/min and 20 mA. All samples appeared to be single phase.

The low-resolution spectra were analyzed with a SPEX DM3000F spectrofluorometer equipped with 0.22 m SPEX 1680 double monochromators (resolution 0.1 nm) and a 450 W xenon lamp as excitation source. The high-resolution emission spectra and decay time were checked with a Spex-1403 spectrophotometer (resolution 0.1 cm^{-1}) under excitation of a N_2 laser beam (337.1 nm) (National Research Instruments Co.) with a flow cryostat of gaseous helium. The temperature can be varied from 10 to 300 K. The high temperature spectra were recorded by a Hitachi MPF-4 spectrophotometer with a 150 W xenon lamp as excitation source and a self-assembled furnace was used as heat source between the temperatures of 300 and 600 K.

3. Results and Discussion

3.1 $BaB_8O_{13}:Sm^{2+}$

The excitation and emission spectra of $BaB_8O_{13}:Sm^{2+}$ are shown in Fig. 1. The excitation of divalent samarium takes place via the strong $4f^55d$ absorption bands from which the ions quickly decay to the lower metastable level $^5D_0$ ($4f^6$). The excitation band peaks at about 28000 cm^{-1}. In the emission spectra, two lines of $^5D_0 \rightarrow {}^7F_0$ transition at 14740 and 14642 cm^{-1} can be observed. They have the strongest intensities which show that divalent samarium occupies a crystallographic site without inversion symmetry in the host. Two crystallographic sites are therefore available for Sm^{2+} in the host lattice even though it was reported that there was only one site in the host [4]. This is in agreement with the results for the crystallographic site in the same host [7]. The other groups of emission lines correspond to the Sm^{2+} $^5D_0$ to ^7F_J ($J = 1, 2$) transitions, respectively. The degeneracy of the $^7F_1$ energy level for both sites is completely lifted and six well-separated lines of the $^5D_0 \rightarrow {}^7F_1$ transition at 14428, 14417, 14365, 14328, 14240, 14189 cm^{-1} are observed. Therefore, the symmetry of the Sm^{2+} site in the host must be lower than C_{2v} because for these symmetries the number of the $^5D_0 \rightarrow {}^7F_0$ transition lines is one, and of the $^5D_0 \rightarrow {}^7F_1$ transition is three [8]. Since the detailed structure of BaB_8O_{13} is still unclear so far and the $^5D_0 \rightarrow {}^7F_2$ transition is not resolved well with sufficient accuracy, the precise symmetry of the Sm^{2+} site cannot be deduced.

Fig. 2 shows the enlargement of the emission spectra of the $^5D_0 \rightarrow {}^7F_0$ transition of Sm^{2+} in BaB_8O_{13} at different temperatures. At 50 K, it can be observed that there are two weak lines at 14592 (denoted as ν) and 14692 cm^{-1} (denoted as ν') which exhibits an about 50 cm^{-1} energy shift together with the $^5D_0 \rightarrow {}^7F_0$ transition at 14642 cm^{-1}. When the temperature increases to 150 K, the intensities of these two lines increase with almost the same energy shift. It also shows that the intensities of the vibronic lines increase with temperature. The lines ν and ν' can be assigned to the phonon satellite

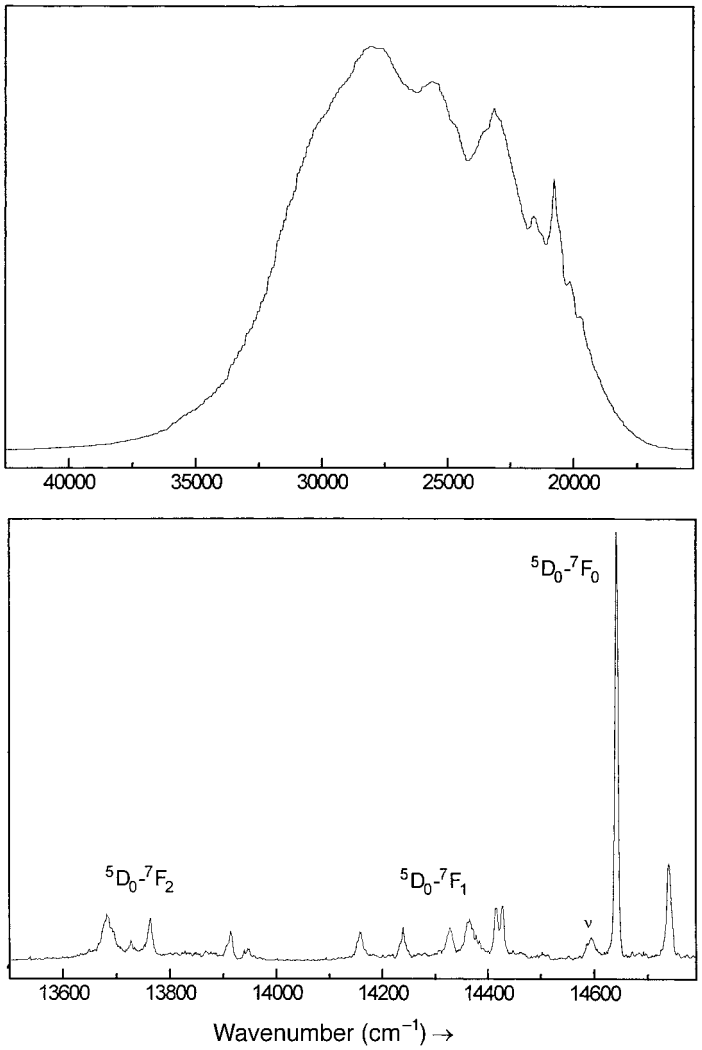

Fig. 1. The low-resolution excitation (λ_{em} = 682 nm) spectrum at room temperature and high-resolution emission spectrum of Sm^{2+} in BaB_8O_{13} at 50 K

lines which were ascribed to electron–phonon coupling with the zero-phonon line (ZPL) ($^5D_0 \rightarrow {}^7F_0$). The vibronic lines ν and ν' can be attributed to the transitions $|^5D_0, n\rangle \rightarrow |^7F_0, n+1\rangle$ (Stokes vibronic) and $|^5D_0, n+1\rangle \rightarrow |^7F_0, n\rangle$ (anti-Stokes vibronic), respectively, where n is the quantum number of vibrational levels of the crystal lattice. The vibration involved is a vibrational mode in which Sm is moved relative to the borate group [9]. The Huang-Rhys factor S (coupling strength) calculated from the relative intensity of the phonon satellite line and the ZP line is about 0.034 [10, 11]. This value is plausible since the 4f electrons are well shielded by the outer $5s^25p^6$ electrons and the electron–phonon coupling would be weak.

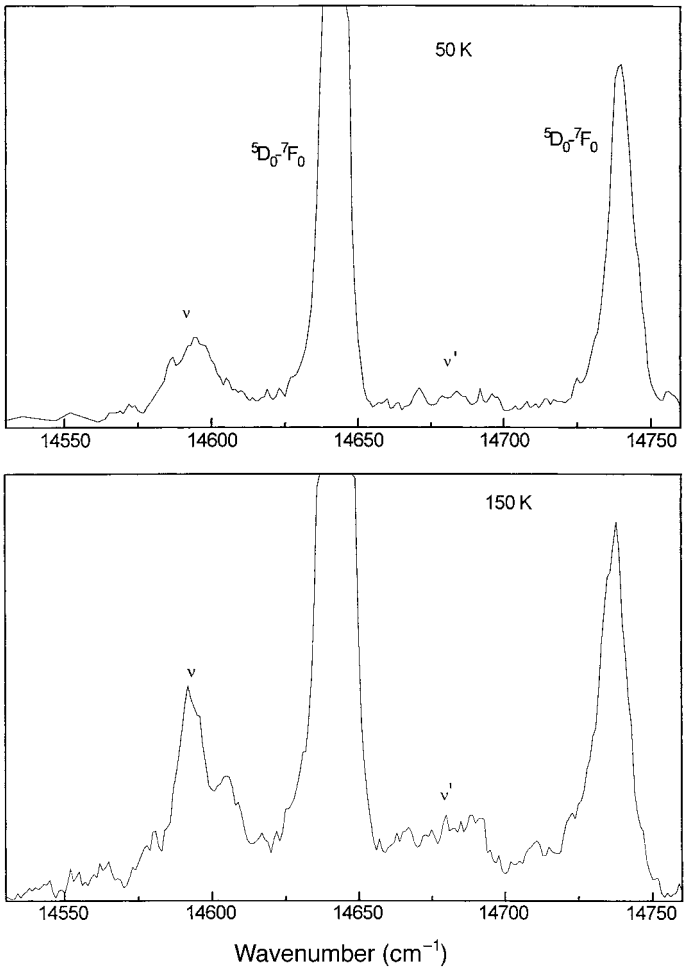

Fig. 2. Enlargement of the high-resolution spectra of the $^5D_0 \rightarrow {}^7F_0$ transition of Sm^{2+} in BaB_8O_{13} at different temperatures

3.2 SrB_4O_7: Sm^{2+}

The excitation and emission spectra of Sm^{2+} in SrB_4O_7 are shown in Fig. 3. The excitation spectrum consists of two bands with maximum at about 27450 and 20400 cm^{-1}, respectively, together with some sharp lines in the band. From the position of the two excitation bands, it is suggested that the $4f^55d$ levels of Sm^{2+} in SrB_4O_7 are located at relatively higher energy than in alkaline earth halides [12 to 14]. In SrB_4O_7, the strontium (and Sm^{2+}) coordination is irregular (C_s) [15] but can be approximated by C_{4v} symmetry, since eight of the nine coordinating oxygen atoms are approximately on the corner of the cube, and the ninth is on one of the tetragonal axes [16]. To assign the bands we should take into account both the crystal-field splitting of the 5d electron and additional splitting of the $4f^5$ configuration. In cubic coordination, the 5d level is split into a lower e_g and a higher t_{2g} level by the crystal

field. The crystal-field splitting of 5d for Sm^{2+} in this host is about 7000 cm^{-1} which is close to the crystal-field splitting of Sm^{2+} in cubic coordination [17]. Since the splitting of the $4f^5$ configuration was well known in the spectroscopy of the Sm^{3+} free ion [18], similarities in the spectra of Sm^{2+} in the present case are expected and therefore, the lines in the spectrum correspond to the ^6H_J (J = 13/2, 11/2, 9/2, 7/2) states of the $4f^5$ configuration.

In the emission spectra, it is found that the dominant line is at about 14567 cm^{-1} which corresponds to the $^5D_0 \rightarrow {}^7F_0$ transition of Sm^{2+} and it shows that the Sm^{2+} ion occupies a site without central symmetry in Sr^{2+}, viz. C_s. The numbers of the transition lines for $^5D_0 \rightarrow {}^7F_J$ are 1, 3, 5 for J = 0, 1, 2, respectively. This is in good agreement with the theoretical splitting of the ^7F_J levels into a maximum of 1, 3 and 5 sublevels for the site symmetry of C_s in this host [8].

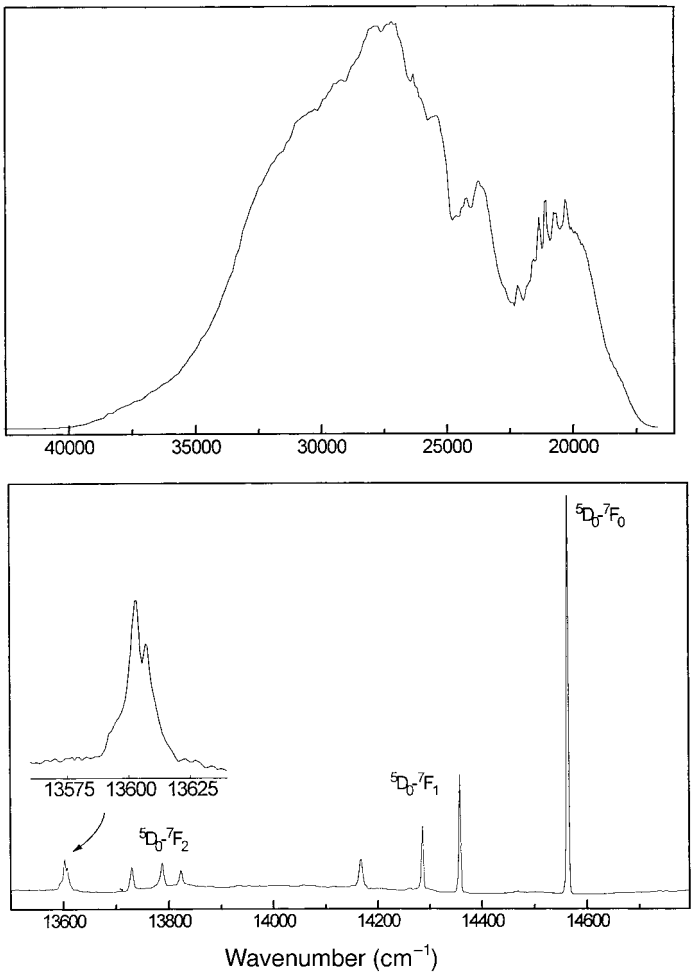

Fig. 3. The low-resolution excitation (λ_{em} = 685 nm) spectrum at room temperature and high-resolution emission spectrum of Sm^{2+} in SrB_4O_7 at 10 K

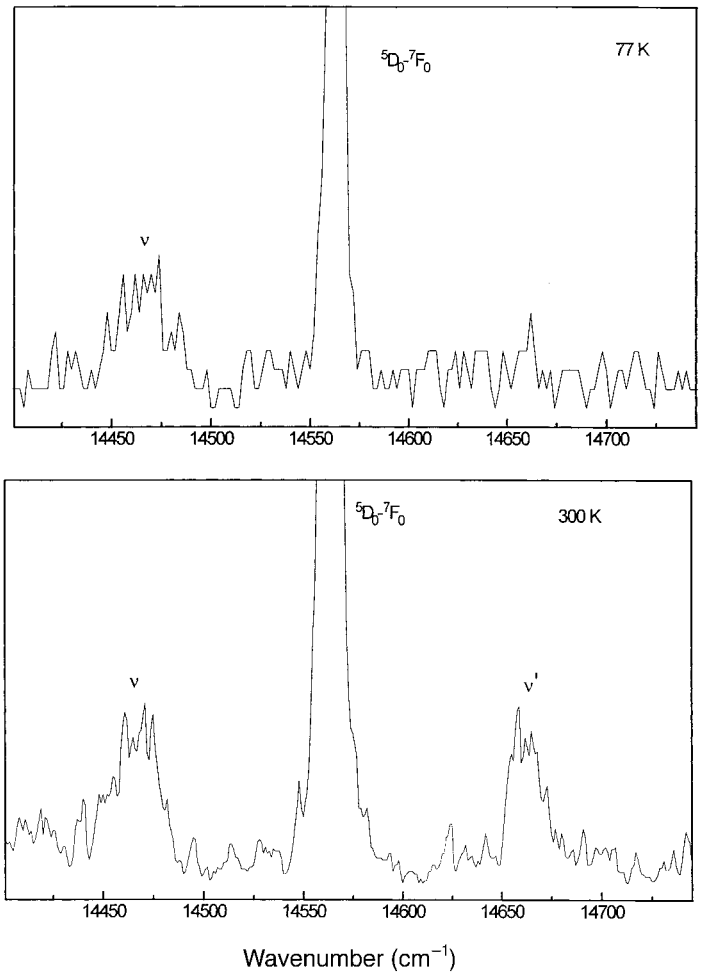

Fig. 4. Enlargement of the high-resolution emission spectra of the $^5D_0 \rightarrow {}^7F_0$ transition of Sm^{2+} in SrB_4O_7 at different temperatures

Fig. 4 shows the enlargement of the emission spectra of the $^5D_0 \rightarrow {}^7F_0$ transition of Sm^{2+} in SrB_4O_7 at 77 and 300 K. Two weak lines which were denoted as ν and ν' (lower and higher-energy side, respectively of the $^5D_0 \rightarrow {}^7F_0$ line) are ascribed to the vibronic emission transition. The energy displacement with the zero-phonon line $^5D_0 \rightarrow {}^7F_0$ (ZPL) is about 95 cm^{-1}. This shows that the $^5D_0 \rightarrow {}^7F_0$ transition of Sm^{2+} couples with a low energy Sm–O vibration and not with the high-energy borate vibration. The Huang-Rhys factor S calculated from the relative intensity of the phonon satellite line and the ZP line is about 0.018. As it is shown in Fig. 4, the intensities of the vibronic lines increase with temperature.

3.3 $SrB_6O_{10}:Sm^{2+}$

The excitation and emission spectra of Sm^{2+} in SrB_6O_{10} are shown in Fig. 5. The excitation band consists of two bands with maxima at about 27400 and 20900 cm^{-1}. Its shape

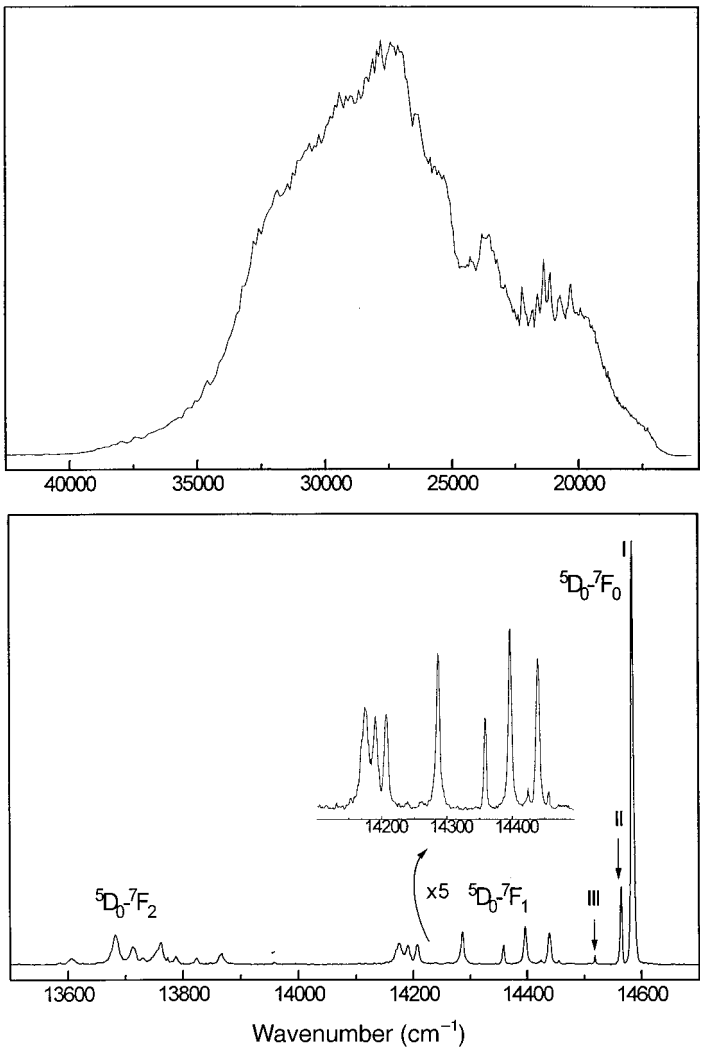

Fig. 5. The low-resolution excitation (λ_{em} = 687 nm) spectrum at room temperature and high-resolution emission spectrum of Sm^{2+} in SrB_6O_{10} at 10 K

is almost identical to that of $SrB_4O_7:Sm^{2+}$. The emission spectrum consists of three groups of lines. The line at 14586 cm^{-1} has the strongest intensity which corresponds to the $^5D_0 \rightarrow {}^7F_0$ transition and it also shows that the Sm^{2+} ion also occupies a site without central symmetry in this host. The other two groups of lines correspond to the $^5D_0 \rightarrow {}^7F_1$ and $^5D_0 \rightarrow {}^7F_2$ transitions. It can be seen that the number of the transition lines for the $^5D_0 \rightarrow {}^7F_0$ transition is three (designated as I, II and III) and for the $^5D_0 \rightarrow {}^7F_1$ transition is nine. Since if the degeneracy of the $^7F_1$ energy level for one site is completely lifted and the lines are well-separated, the number of its lines are at most three, therefore, there are at least three crystal sites for Sm^{2+} in this host. This confirms the results of [19 to 21] in which the authors assumed that three crystallographic sites

of cations were possible in the host. The $^5D_0 \rightarrow {}^7F_2$ transition lines are not resolved well and therefore no precise site symmetry of Sm^{2+} in this host can be deduced from the luminescence. However, its symmetry must be lower than C_{2v} as Sm^{2+} in the other two borates.

Fig. 6 shows the luminescence of Sm^{2+} in these three borates in the range of 620 to 675 nm at room temperature. Considering the position and line shape, these lines must correspond to the $^5D_1$ to ^7F_J (0, 1, 2) transitions of Sm^{2+}. It is an interesting phenomenon. The vibrational mode of BO_4 and BO_3 is at around 1200 to 1400 cm^{-1} [22] which is very close to the energy gap between $^5D_1$ and $^5D_0$ level ($\Delta E \approx 1350$ cm^{-1}). This energy gap can be bridged by only one phonon. Therefore, the non-radiative transition probability from $^5D_1$ to $^5D_0$ level must be very high and no transitions between $^5D_1$ and ^7F_J could be observed. However, in the present case, $^5D_1 \rightarrow {}^7F_J$ (0, 1, 2) transitions occur even at room temperature. Such observation can be explained assuming that the $^5D_1$ level is thermally populated by the $^5D_0$ level resulting in the transition $^5D_0 \rightarrow {}^5D_1 \rightarrow {}^7F_J$. Such thermal population process is also found in the high-temperature luminescence of Sm^{2+} in this system (see below).

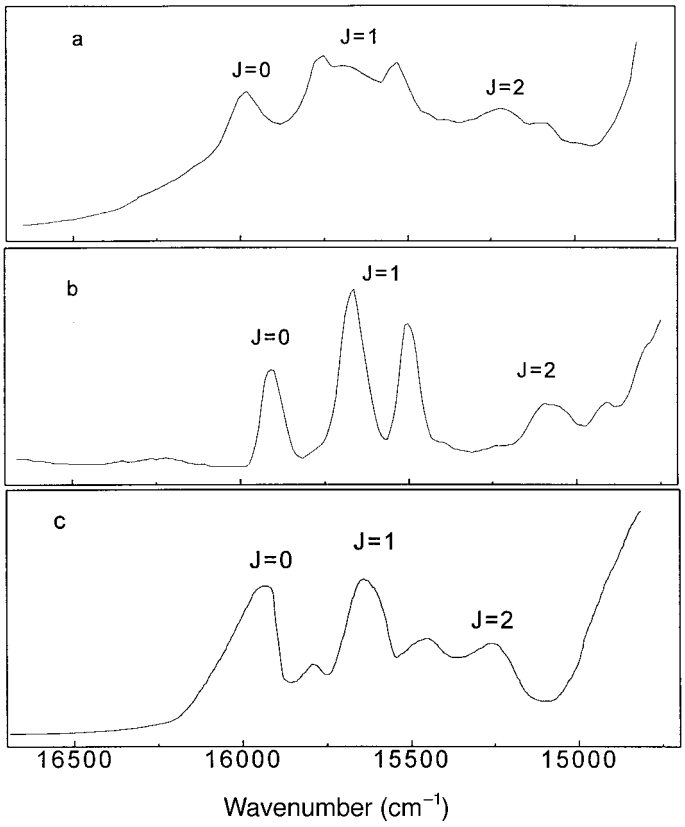

Fig. 6. The low-resolution emission spectra of Sm^{2+} $^5D_1 \rightarrow {}^7F_J$ (J = 0, 1 2) in a) BaB_8O_{13}, b) SrB_4O_7 and c) SrB_6O_{10} at room temperature

3.4 Temperature effects on the luminescence of the $^5D_0 \rightarrow {}^7F_0$ transition of Sm^{2+} in BaB_8O_{13} and SrB_6O_{10}

It was reported that the luminescence of Sm^{2+} in crystalline SrB_4O_7 was not dependent on temperature [23]. Our results show that the temperature effects on the luminescence of Sm^{2+} in this host are not definite and no convincing data are obtained from our experimental set-ups, and therefore, no related information is presented in this paper.

The temperature effects on the line shift of the $^5D_0 \rightarrow {}^7F_0$ transition of Sm^{2+} in BaB_8O_{13} and SrB_6O_{10} are shown in Fig. 7. In $BaB_8O_{13}:Sm^{2+}$, the line of Center II shifts to the higher energy side while the line of Center I shifts to the lower energy side. The line broadens and the transition intensity (Center II) increases with temperature up to 300 K. The line of Center I shifts to the lower energy side with temperature.

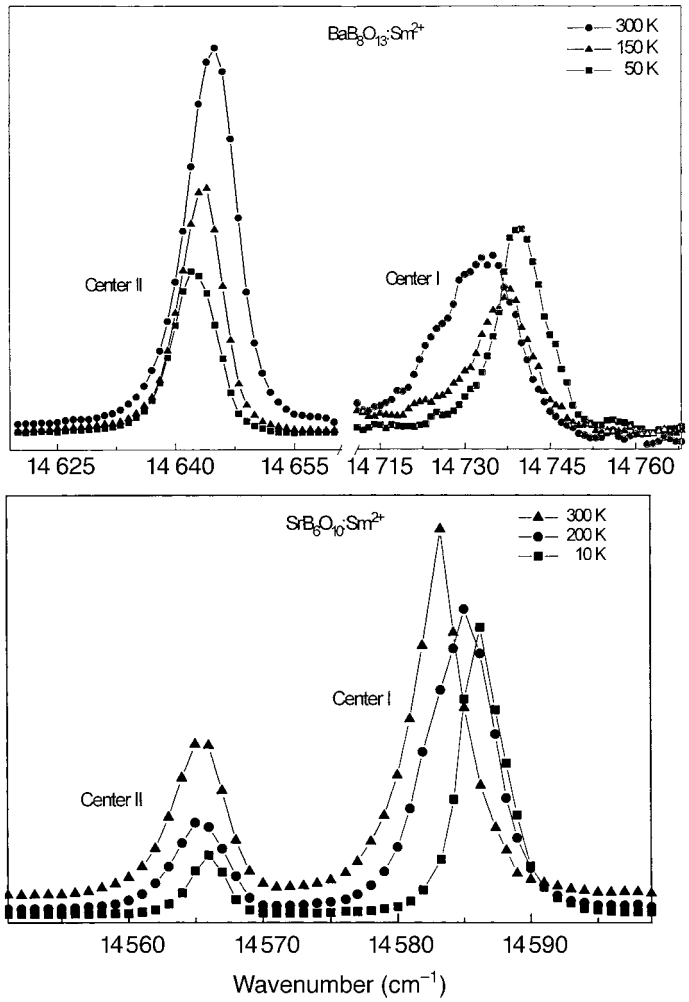

Fig. 7. The temperature effects on the high-resolution emission spectra of Sm^{2+} $^5D_0 \rightarrow {}^7F_0$ in BaB_8O_{13} and SrB_6O_{10}

In $SrB_6O_{10}:Sm^{2+}$, both lines shift to the lower energy side. The intensity ratio of Center II to Center I increases with temperature. In both samples, the line width of the $^5D_0 \rightarrow {}^7F_0$ transition broadens with temperature.

In a qualitative way, the temperature effects on the intensities of the Sm^{2+} $^5D_0 \rightarrow {}^7F_0$ transition can be illustrative for the temperature dependence of the energy migration process between two centers. It is caused by the need of phonon assistance in the energy migration process. Such energy migration process was also observed in divalent europium doped SrB_6O_{10} [19 to 21]. It can also be confirmed by the decay time of these centers as to be discussed in the text below.

3.5 Decay time of the $^5D_0 \rightarrow {}^7F_0$ transition of Sm^{2+} in BaB_8O_{13}, SrB_4O_7 and SrB_6O_{10}

Due to the low intensity of Center II of the Sm^{2+} $^5D_0 \rightarrow {}^7F_0$ transition in BaB_8O_{13} and Center III in SrB_6O_{10}, no data of their decay time are obtained.

The decay curves of the Sm^{2+} $^5D_0 \rightarrow {}^7F_0$ transition in all three borates are single exponential. The decay time for the Sm^{2+} $^5D_0 \rightarrow {}^7F_0$ transition in SrB_4O_7 is about 3.4 ms at 10 K which is close to the results of [23]. The decay time is almost independent of temperature.

The decay time of the Sm^{2+} $^5D_0 \rightarrow {}^7F_0$ transition (Center II) in BaB_8O_{13} shows that the lifetime is also temperature independent at temperatures from 50 to 300 K. At 50 K, the lifetime is $\tau \approx 3.5$ ms and at 200 K, $\tau \approx 3.7$ ms. It seems to be contradictory with the temperature dependence of the emission intensities, as shown above, that the intensities increase with temperature. Theoretically, the decay time should become longer with increasing population number in the $^5D_0$ levels. Such contradiction may be explained by the increase of the radiative decay rate with increasing temperature, therefore, the decrease of the decay time is compensated by this increase and these processes lead to the temperature-independent decay time.

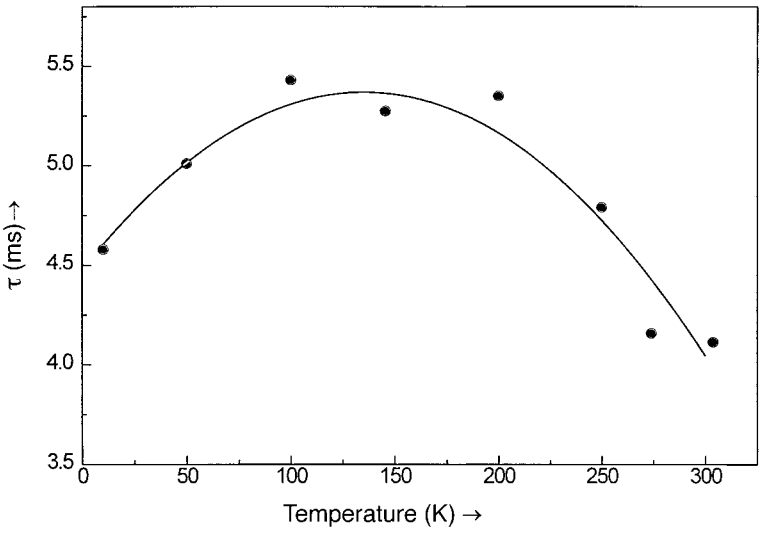

Fig. 8. The temperature dependence of the decay time of the Sm^{2+} $^5D_0 \rightarrow {}^7F_0$ transition in Center I in SrB_6O_{10}

The lifetimes of the Sm^{2+} $^5D_0 \rightarrow {}^7F_0$ transition in SrB_6O_{10} for Center I and II at 10 K are close to each other, $\tau_I \approx 5.0$ ms, $\tau_{II} \approx 4.5$ ms. But at 300 K, the lifetimes for these two centers are 4.24 and 2.69 ms, respectively. Due to their different decay time, it can be deduced that these two emissions originate from different luminescent centers.

The dependence of the lifetime of Center I of Sm^{2+} in SrB_6O_{10} on temperature in the range of 10 to 300 K is plotted in Fig. 8. It shows that the decay time of Sm^{2+} in Center I is temperature-dependent. The decay time generally decreases with temperature. The decay time presents a small rise at low temperature, which was possibly due to the energy transfer from Center III to Center II and Center I. The decay time starts decreasing at about 150 K. Thereafter, the decay time decreases with temperature due to the thermal depopulation in the $^5D_0$ level. This agrees with reports on the luminescence of Eu^{2+} in this host [19 to 21]. Those authors reported that the luminescence of Eu^{2+} in Center III is almost quenched at 150 K. In our case, we also find that the intensities of the luminescence of $^5D_0 \rightarrow {}^7F_J$ (J = 0, 1, 2) in Center III decrease with temperature from 10 K and its energy might be transferred to Center I (or Center II).

3.6 The luminescence of Sm^{2+} at high temperature

Fig. 9 shows the luminescence of Sm^{2+} in these three borates at 450 K. Some difference can be found among the luminescence of Sm^{2+}. There is a broad band with maximum at about 575 to 580 nm for the emission of Sm^{2+} in SrB_4O_7 and SrB_6O_{10} whereas no such broad band is found in BaB_8O_{13}. This band is assigned to the 4f → 5d transition of Sm^{2+}.

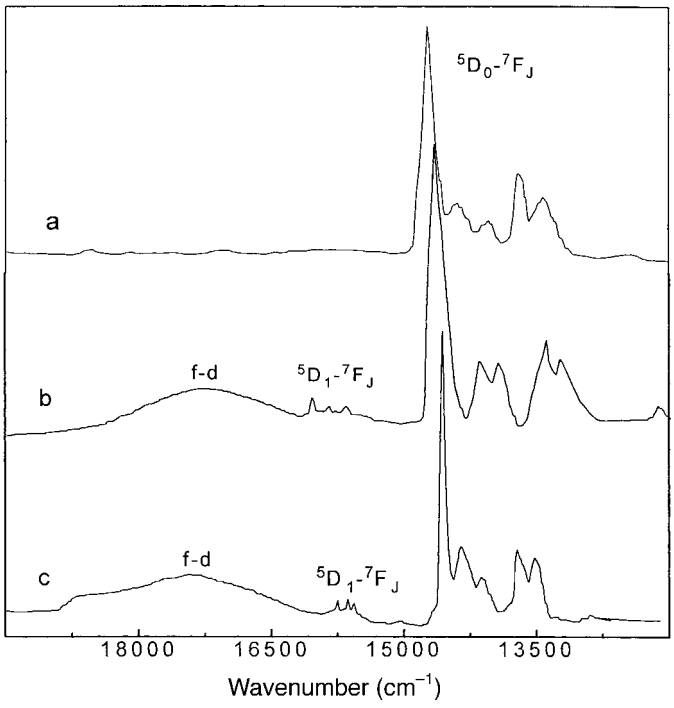

Fig. 9. The low-resolution emission spectra of Sm^{2+} in a) BaB_8O_{13}, b) SrB_4O_7 and c) SrB_6O_{10} at 450 K

The intensities of the band emission increase with increasing temperature and that of $^5D_0 \rightarrow {}^7F_J$ transitions decrease. These results are in conflict with the two-step fluorescence quenching mechanism [24] in which generally, the $^5D_1 \rightarrow {}^7F_J$ ($J = 0, 1, 2$) transitions are quenched earlier by temperature before this occurs for the $^5D_0 \rightarrow {}^7F_J$ ($J = 0, 1, 2$) transitions. If we take a look at the excitation spectra of Sm^{2+} in BaB_8O_{13}, SrB_4O_7 and SrB_6O_{10}, we can find that the excitation spectra of Sm^{2+} in SrB_4O_7 and SrB_6O_{10} consist of two broad strong bands with the lowest energy at about 20200 cm^{-1} while only of one broad band in the excitation spectrum in BaB_8O_{13} with energy at about 28000 cm^{-1}. The emission spectra also show that the $^5D_0$ level of Sm^{2+} in BaB_8O_{13} at 14645 cm^{-1} is higher than in SrB_4O_7 at 14567 cm^{-1} and SrB_6O_{10} at 14586 cm^{-1}. Therefore, the lowest lying energy level of $4f^55d$ must be closer to the $^5D_0$ level in SrB_4O_7 and SrB_6O_{10} than in BaB_8O_{13} and the electrons in the $^5D_0$ level are easier to be pumped by temperature to the $4f^55d$ level and lead to a broad band emission at high temperature. Therefore, the appearance of the $4f^55d \rightarrow 4f^6$ transition at room temperature and its increase in intensity with increasing temperature is then due to the thermal population of the $^5D_1$ level by the $^5D_0$ level. In fact, the mechanism of the appearance of $^5D_1$ to ^7F_J transitions is the same as that of the $4f^55d \rightarrow 4f^6$ transition, but since the $4f^55d \rightarrow 4f^6$ is a parity-allowed transition, its intensity is then much higher than that of $^5D_1 \rightarrow {}^7F_J$ parity-forbidden transitions.

4. Conclusions

The luminescence of Sm^{2+} in alkaline earth borates (BaB_8O_{13}, SrB_4O_7 and SrB_6O_{10}) shows that Sm^{2+} occupies a site without central symmetry. Two crystallographic sites for Sm^{2+} in BaB_8O_{13} and three in SrB_6O_{10} are evidenced by the high-resolution emission spectra at low temperature. Energy migration between the crystallographic sites for Sm^{2+} in BaB_8O_{13} and SrB_6O_{10} is possible. Due to the thermal population, the $^5D_1 \rightarrow {}^7F_J$ transitions are observed at room temperature even though the vibration of borate is a high-frequency one. The f–d transitions of Sm^{2+} in SrB_4O_7 and SrB_6O_{10} are observed at high temperature due to the lower energy position of the $4f^55d$ level and the small energy difference between $4f^55d$ and $^5D_0$ levels. The decay time of Sm^{2+} in SrB_4O_7 and BaB_8O_{13} is temperature-independent while it is temperature-dependent in SrB_6O_{10}. All the decay curves are single exponential.

The study on the temperature dependence of luminescence of Sm^{2+} in BaB_8O_{13}, SrB_6O_{10} and SrB_4O_7 shows that the temperature variation of Sm^{2+} fluorescence is most probably governed by the lowest lying $4f^55d$ states and the 5d Stark levels are affected by the crystal field more seriously than 4f states. At each temperature the intensity of the fluorescent lines originating from each state is determined by the population of the state and by the probability for spontaneous decay. As a result, when describing the temperature dependence of Sm^{2+} fluorescence in the series of similar lattices, the variation of the f–d energy gap as well as the usual dependence on the mediating phonon frequency must be taken into account. In our experiments, no f–d transition of Sm^{2+} in BaB_8O_{13} is observed at temperatures from 10 to 573 K. This is because the $4f^55d$ level is located at a relatively higher energetic position than in SrB_4O_7 and SrB_6O_{10}.

Acknowledgements This work was supported by the National Key Project for Fundamental Research, National Nature Science Foundation of China and Laboratory of Excited State Processes of the Chinese Academy of Sciences.

References

[1] G. Blasse, Internat. Rev. Phys. Chem. **11**, 71 (1992).
[2] A. Ellens, H. Andres, M. Ter Heerdt, A. Meijerink, and G. Blasse, J. Lum. **66/67**, 240 (1996).
[3] G. Blasse, Inorg. Chim. Acta **167**, 33 (1990).
[4] B. Di Bartolo, Optical Interaction in Solids, John Wiley & Sons, New York 1968 (p. 356).
[5] J. Krogh-Moe, Acta Cryst. **B25**, 2153 (1969).
[6] C. F. Chenot, J. Amer. Cerem. Soc. **50**, 117 (1967).
[7] T. Koskentalo, L. Niisto, and G. Blasse, J. Less-Common Metals **112**, 67 (1985).
[8] S. Zhang, Lum. Display Devices **4**, 12 (1982) (in Chinese).
[9] J. Verwey, G. Dirksen, and G. Blasse, J. Phys. Chem. Solids **53**, 367 (1992).
[10] K. Huang and C. Rhys, Proc. Roy. Soc. (London) A **204**, 406 (1950).
[11] S. Pekar, Zh. Eksper. Teor. Fiz. **20**, 510 (1950).
[12] H. V. Lauer, Jr. and F. K. Fong, J. Chem. Phys. **65**, 3108 (1976).
[13] A. Gros, F. Gaume, and J. C. Gacon, J. Solid State Chem. **36**, 324 (1981).
[14] P. P. Sorokin, M. J. Stenvenson, J. R. Lank, and G. D. Pettit, Phys. Rev. **127**, 503 (1962).
[15] A. Perloff and S. Block, Acta Cryst. **20**, 274 (1966).
[16] G. Blass, G. J. Dirksen, and A. Meijerink, Chem. Phys. Lett. **167**, 41 (1990).
[17] A. Meijerink and G. J. Dirksen, J. Lum. **63**, 189 (1995).
[18] G. H. Dieke, Spectra and Energy Levels of Rare Earth Ions in Crystals, Eds. H. M. Crosswhite and H. Crosswhite, Wiley, New York 1968.
[19] K. Machida, G. Adachi, and J. Shiokawa, J. Lum. **21**, 101 (1979).
[20] M. Leskla, T. Koskentalo, and G. Blasse, J. Solid State Chem. **59**, 272 (1985).
[21] W. Schipper, D. Voort, P. Berg, Z. Vroon, and G. Blasse, Mater. Chem. Phys. **33**, 311 (1993).
[22] C. E. Weir and P. A. Schroeder, J. Res. NBS **68**A, 465 (1964).
[23] J. W. M. Verwey, G. J. Dirksen, and G. Blasse, J. Phys. Chem. Solids **53**, 367 (1992).
[24] H. V. Lauer, Jr. and F. K. Fong, J. Chem. Phys. **65**, 3108 (1976).